

## **Supporting Information**

### **Next generation miRNA inhibition using short anti-seed PNAs encapsulated in PLGA nanoparticles**

Shipra Malik<sup>1</sup>, Jihoon Lim<sup>2</sup>, Frank J Slack<sup>2</sup>, Demetrios T Braddock<sup>3</sup>, Raman Bahal<sup>1\*</sup>

<sup>1</sup>Department of Pharmaceutical Sciences, University of Connecticut, Storrs, CT, 06269, USA

<sup>2</sup>Department of Pathology, BIDMC Cancer Center, Harvard Medical School, 330 Brookline Ave,  
Boston, MA 02215, USA

<sup>3</sup>Department of Pathology, Yale University School of Medicine, 310 Cedar Street, New Haven  
CT, 06510, USA

**Table 1.** MALDI analysis of PNA oligomers employed in this study. Calculated molecular weight (MW) was provided and observed MW was assessed using MALDI-TOF analysis.

<b>PNA</b>	<b>Calculated MW (Daltons, Da)</b>	<b>Observed MW (Daltons, Da)</b>
PNA 1	2305.6	2308.8
PNA 2	2693.1	2695.3
PNA 3	2994.2	2997.2
PNA 4	2994.2	2998.2
PNA 5	6770.4	6784.9
PNA 6	2764.1	2763.9
PNA 7	3312.6	3309.1
PNA 8	3424.7	3425.6
PNA 9	3424.7	3421.7
PNA 10	6918.3	6922.1
PNA 11	7389.9	7391.1

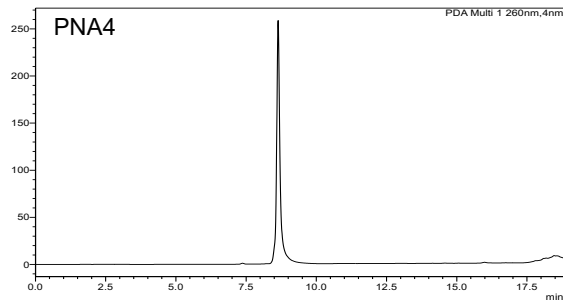
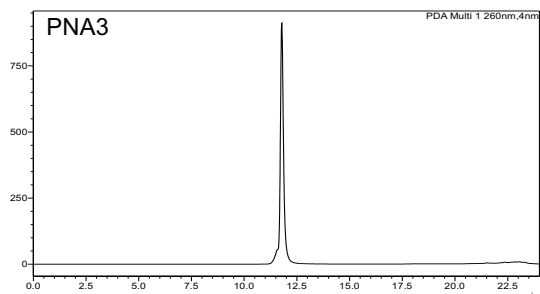
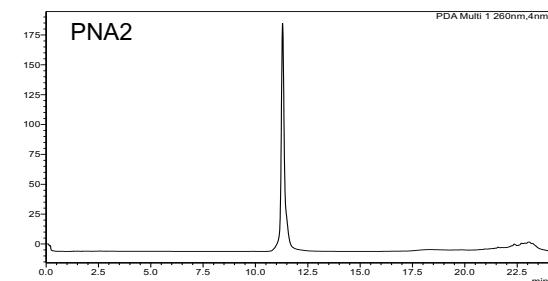
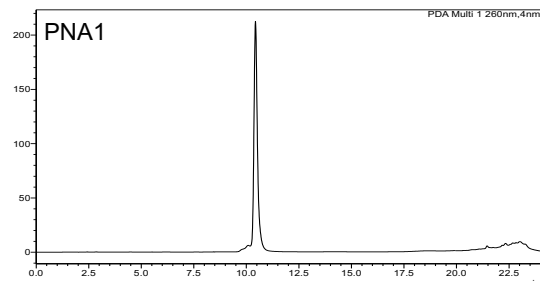


**Figure S1.** HPLC profiles of synthesized PNAs 1-4.

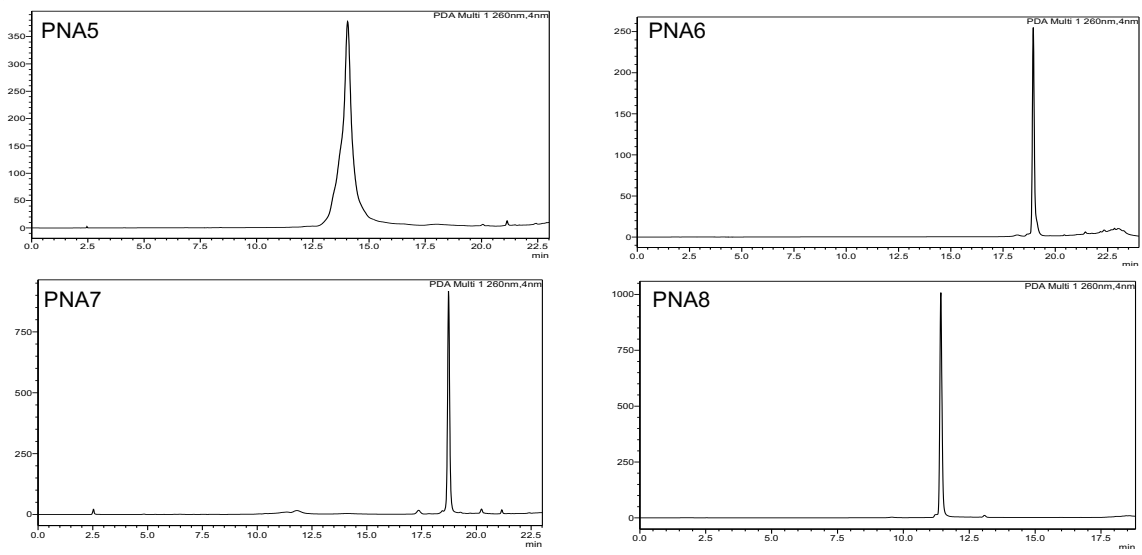


**Figure S2.** HPLC profiles of synthesized PNAs 5-8.



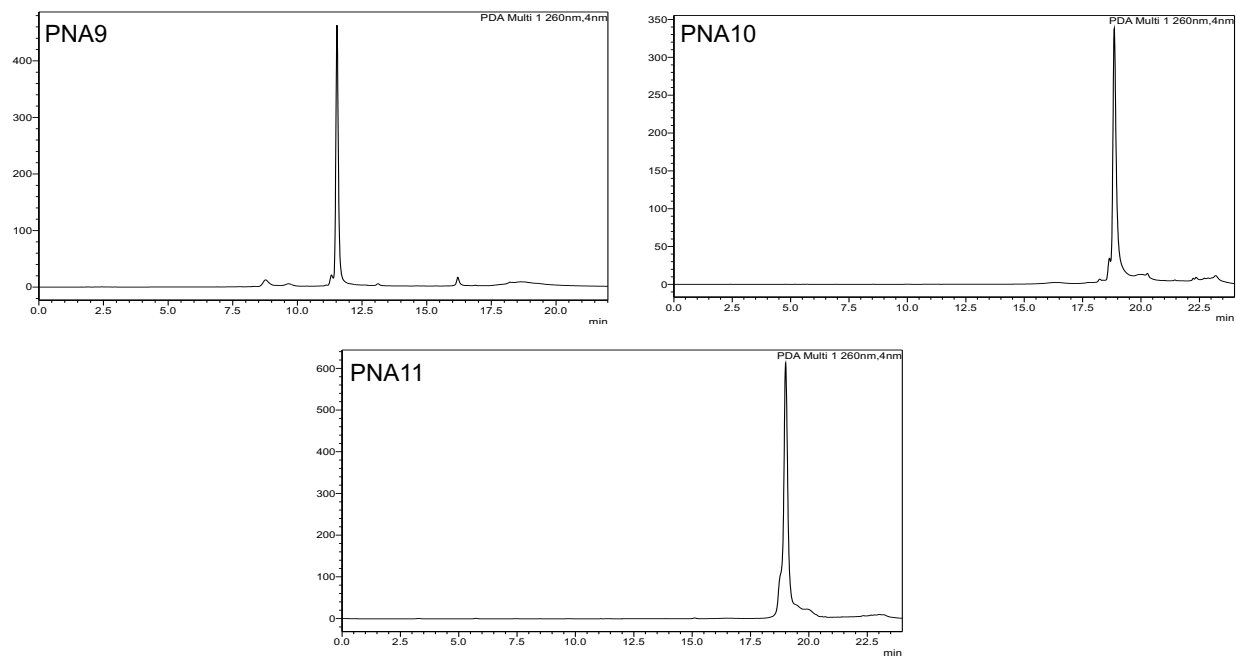


**Figure S3.** HPLC profiles of synthesized PNAs 9-11.

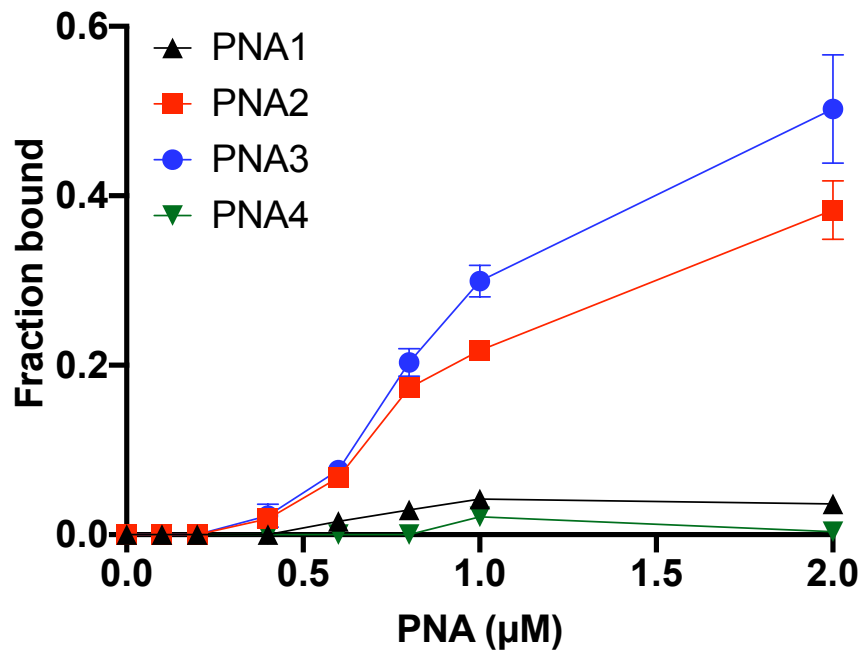


**Figure S4.** Graph representing the bound fraction of PNAs 1, 2, 3 and 4 after incubation with the target miR-155 (1.0  $\mu\text{M}$ ) at different concentrations in simulated physiological buffer conditions (10 mM NaPi, 150 mM KCl, and 2 mM  $\text{MgCl}_2$ ) for 1 hour at 37°C followed by non-denaturing PAGE separation and SYBR Gold staining. PNA3 shows higher bound fraction in comparison to PNA2 and PNA1. PNA4 is the scramble control and does not show any binding to the target.

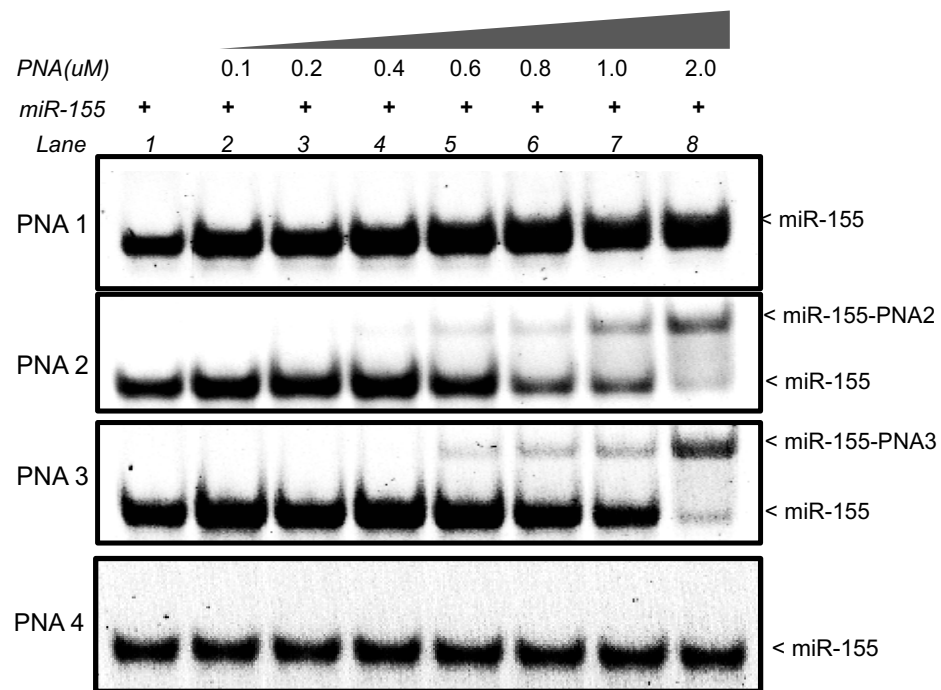


**Figure S5.** Dose dependent gel-shift assay of miR-155 target and indicated short PNA probes after 16 hours of incubation. Incubations were performed in simulated physiological buffer conditions (10 mM NaPi, 150 mM KCl, and 2 mM MgCl<sub>2</sub>) for 16 hours at 37°C followed by non-denaturing PAGE separation and SYBR Gold staining.

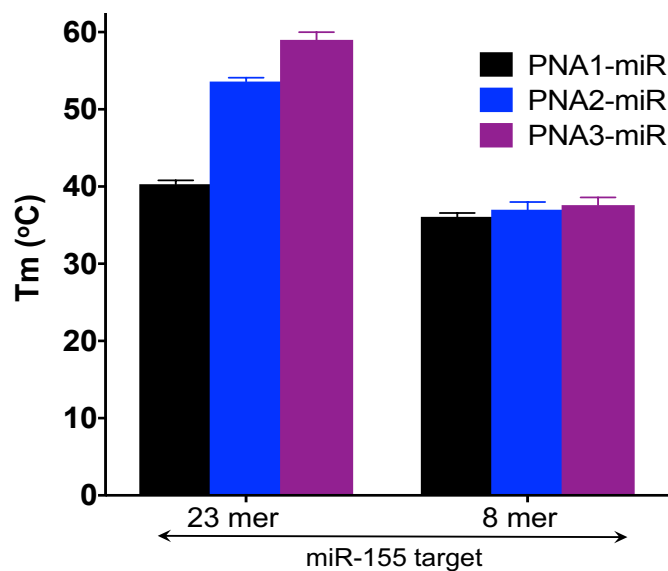


**Figure S6.** Comparative analysis of thermal denaturation temperature ( $T_m$ ) of PNAs-miR-155 duplex's measured by UV-melting studies. PNAs were annealed with full length miR-155 (23 mer) and short length (8mer) miR-155. The concentration of each strand was 4  $\mu$ M, prepared in simulated physiological buffer and pH 7.4 conditions. Both the heating and the cooling runs were recorded, with both runs showing nearly identical profiles. The  $T_m$ s were determined by taking the first derivative of the melting curves.  $n=3$  for each sample, data represented as mean  $\pm$  SEM.

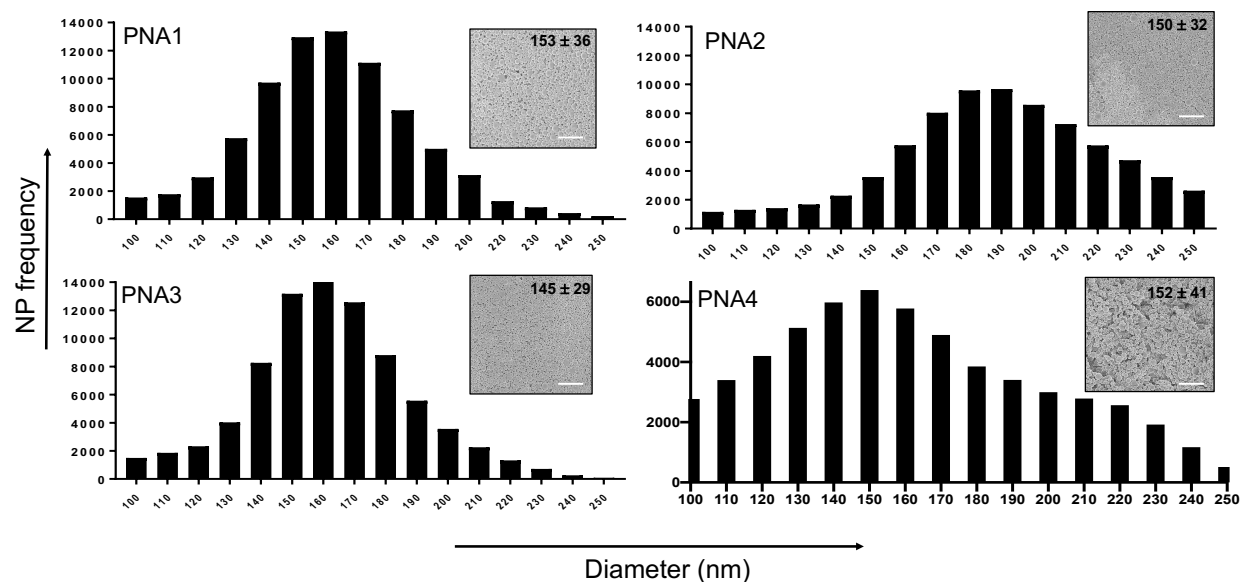


**Figure S7.** Representative size distribution and scanning electron micrographs (SEM) (inset) of PLGA nanoparticles containing short PNA probes. Scale bar represents 1  $\mu\text{m}$ . Average particle diameter (nm) and SD are given for each nanoparticle batch.

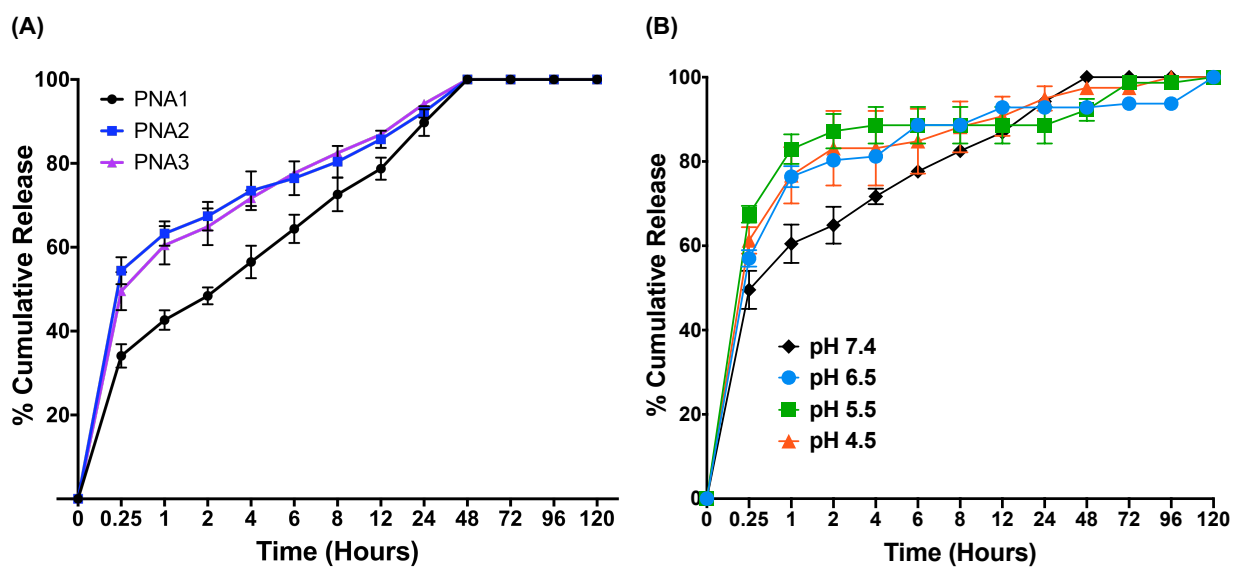


**Figure S8. (A)** Graph representing the percentage cumulative release of PNA 1, 2, and 3 from PLGA NPs at pH 7.4. The results are represented as mean $\pm$ SEM (n=3). **(B)** Graph representing percentage cumulative release of PNA3 NPs in different pH conditions including pH 7.4, 6.5, 5.5 and 4.5. The results are represented as mean $\pm$ SEM (n=3).

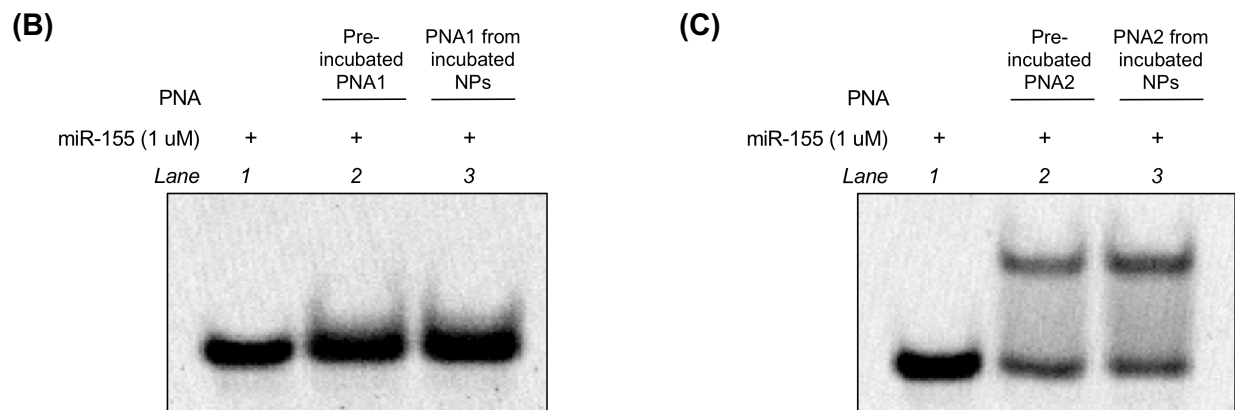
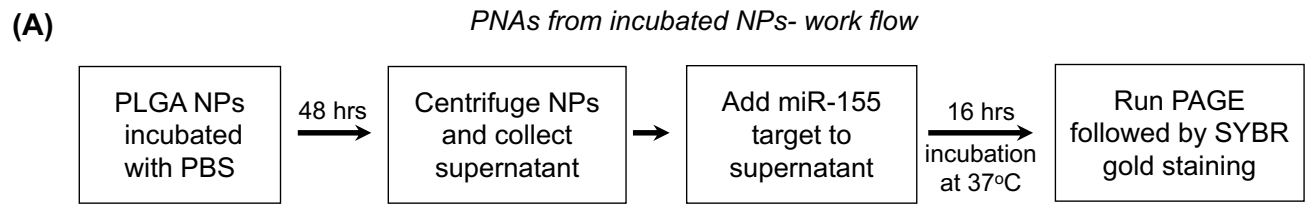


**Figure S9.** (A) Schematic showing work flow to evaluate the release and assessing the *in vitro* binding affinity of PNAs with target miR-155. (B) Gel-shift assay following incubation of miR-155 target (1.0  $\mu$ M) with PNA1 (pre-incubated) and PNA1 released from PLGA NPs in simulated physiological salt conditions at 1:1 ratio. (C) Gel-shift assay following incubation of miR-155 target (1.0  $\mu$ M) with PNA2 (pre-incubated) and PNA2 released from PLGA NPs in simulated physiological salt conditions at 1:1 ratio.

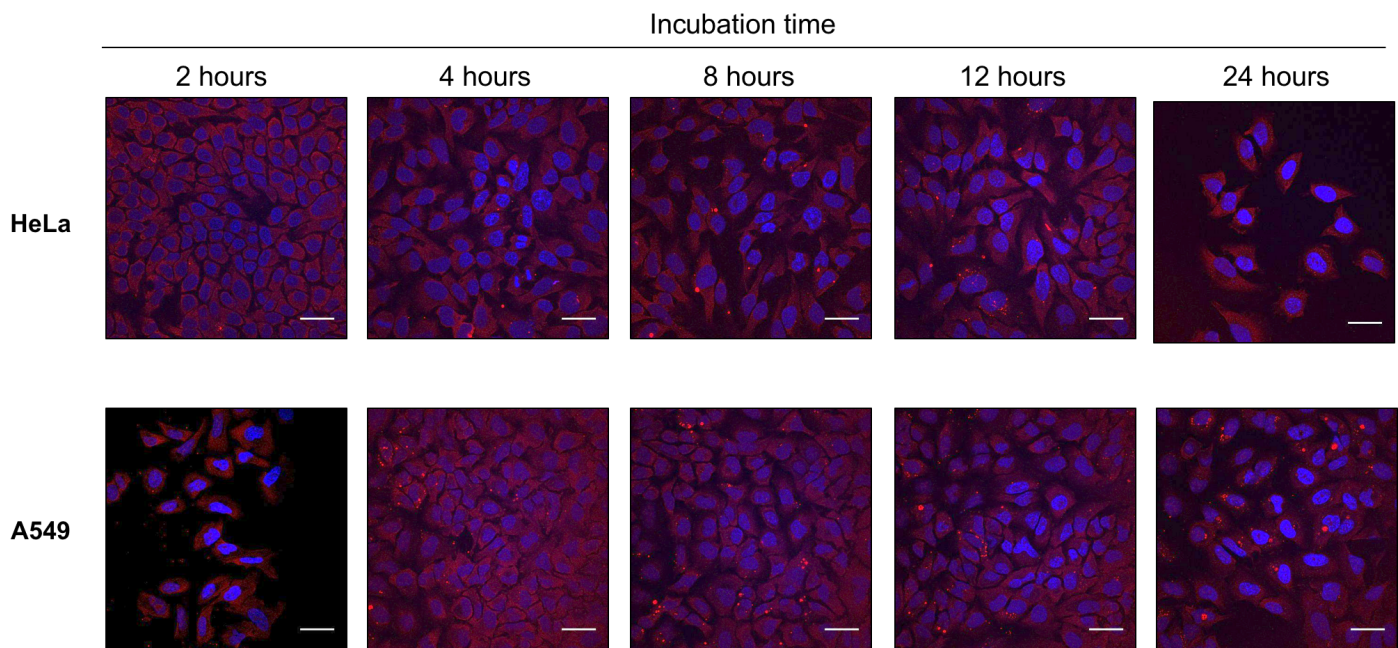


**Figure S10.** Fluorescent images of HeLa (top panel) and A549 (bottom panel) cells incubated with PLGA NPs containing PNA8 (1 nmol PNA dose) after 2, 4, 8, 12, and 24 hours. Blue (DAPI) indicates nucleus and red indicates TAMRA. Scale bar represents 30  $\mu\text{m}$ .



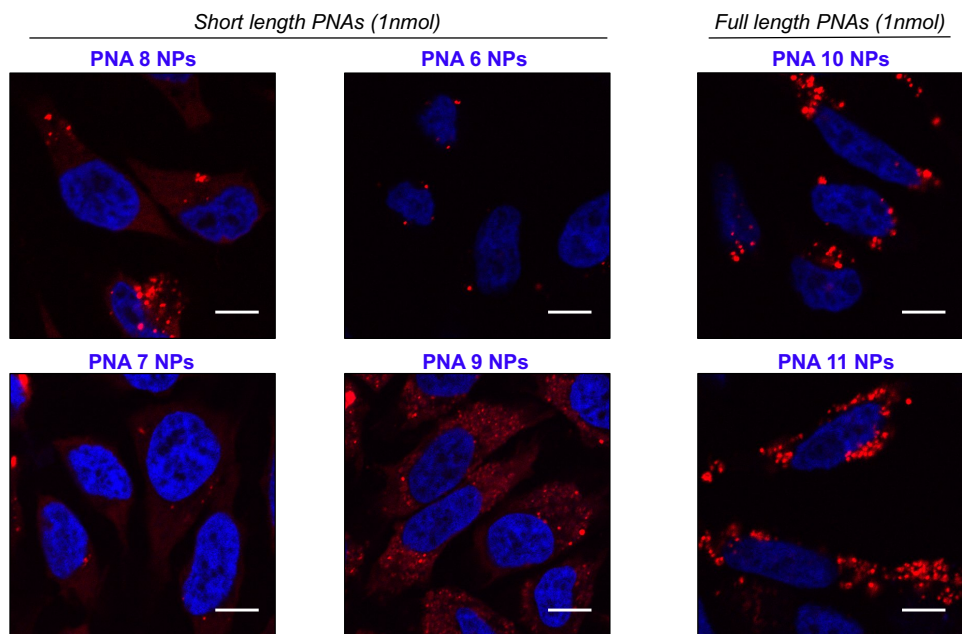


**Figure S11.** Fluorescent images of HeLa cells incubated with PLGA NPs containing indicated PNAs (1 nmol PNA equivalent dose). HeLa cells were incubated with PLGA NPs for 24 hours, followed by brief washing with PBS and incubation with DAPI (nuclear staining). Blue (DAPI) indicates nucleus and red indicates TAMRA. PLGA NPs containing short length arginine or lysine conjugated PNAs (PNA7, PNA8, and PNA9) show more diffused distributions whereas PLGA NPs containing regular short PNA6 show more puncta. PLGA NPs containing long length PNAs (PNA10 and PNA11) demonstrate both puncta as well as diffused pattern of TAMRA dye. Scale bar represents 10  $\mu\text{m}$ .

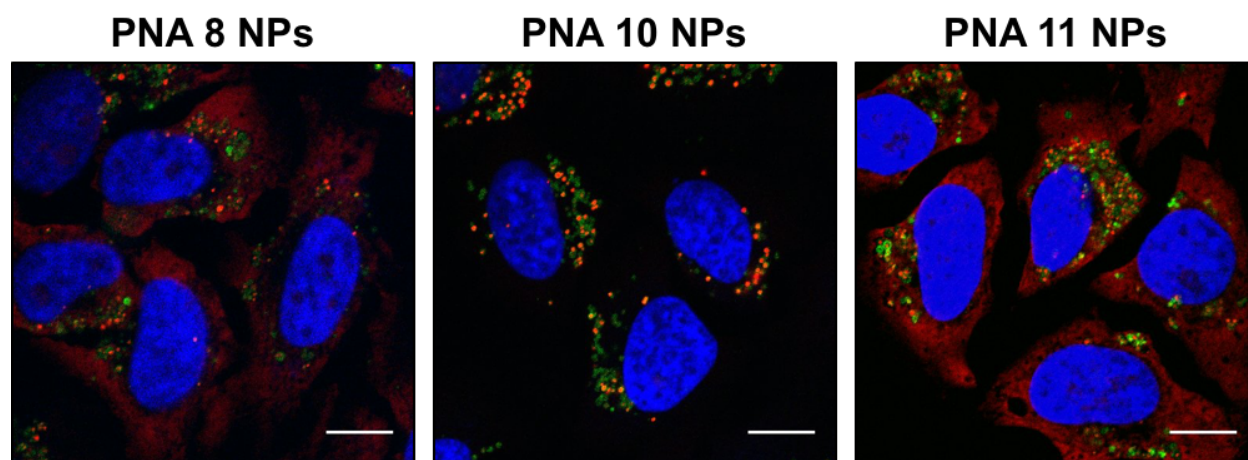


**Figure S12.** Fluorescent images of HeLa cells incubated with PLGA NPs containing indicated PNAs (8, 10, and 11) at 1 nmol PNA equivalent dose after 24 hours. Treated HeLa cells were incubated with lysotracker (200  $\mu$ M) at 37°C and 5% CO<sub>2</sub> for 40 minutes. Cells were then washed, fixed using 4% PFA, and permeabilized followed by staining of nucleus with DAPI. Blue (DAPI) indicates nucleus, green indicates lysotracker, red indicates TAMRA. PNA8 and PNA11 NPs show accumulation in lysosomes as well as cytosolic distribution, however PNA10 NPs are present only in the lysosomes. Scale bar represents 10  $\mu$ m.

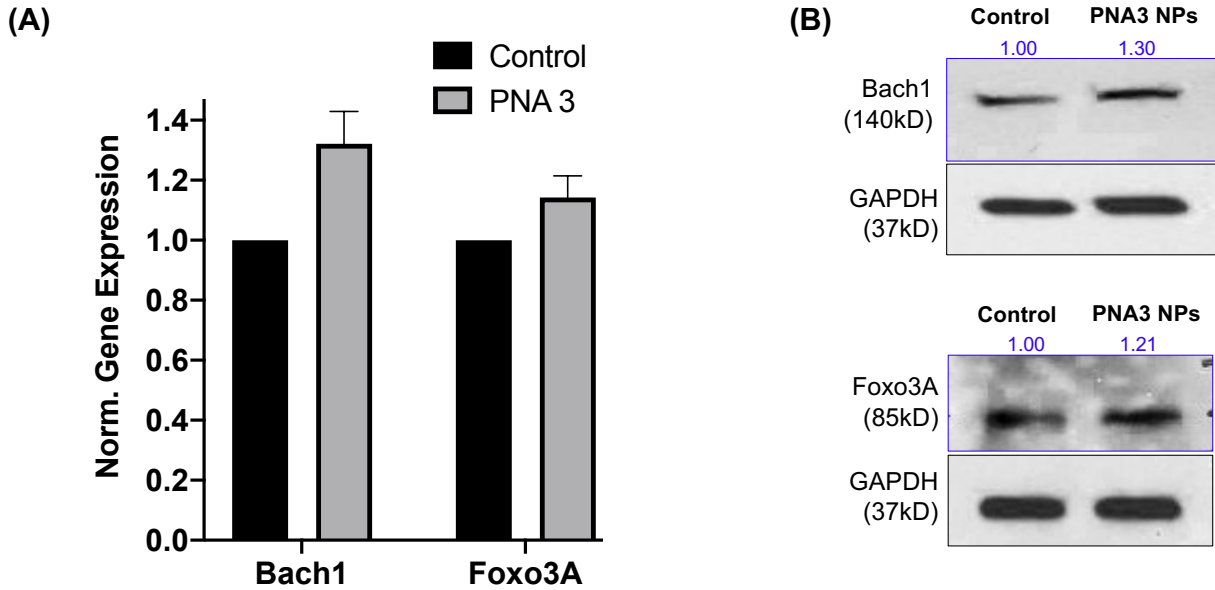
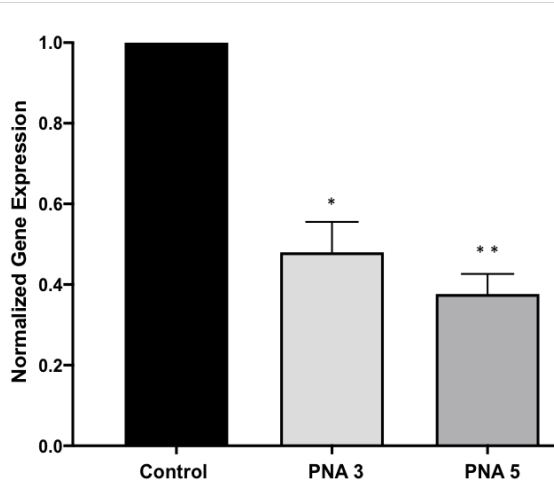


**Figure S13.** (A) Relative miR-155 downstream targets; BACH1 and FOXO3A gene expression levels in RNA extracted from SUDHL-5 cells treated with PLGA NPs containing PNA3 at 2.5 nmol of PNA equivalent dose ( $n = 3$ , data represented as mean  $\pm$  SEM). One sample t and Wilcoxon test was used for statistical analysis. (B) Western blot of downstream target protein extracted from SUDHL-5 cell lines treated with the PLGA NPs containing PNA3 at 2.5 nmol of PNA equivalent dose.

(A)



(B)

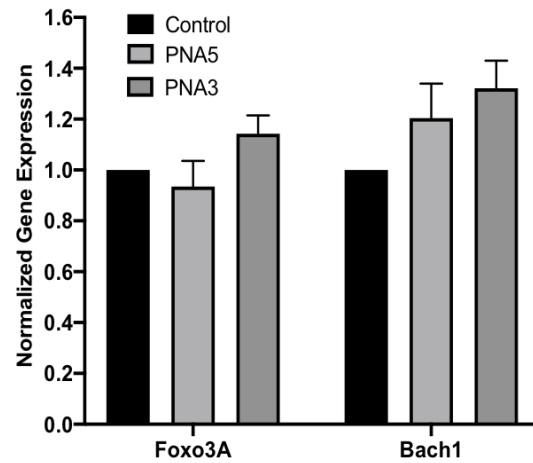


**Figure S14.** (A) Relative miR-155 gene expression in SUDHL-5 cells after treatment with NPs containing 8mer PNA3 and 23mer PNA5 (2.5 nmol PNA equivalent dose). miR-155 expression relative to average control (all normalized to U6, n = 3, \*p < 0.05, \*\* p < 0.005). (B) The relative expression of downstream targets of miR-155 (BACH1 and FOXO3A) in SUDHL-5 cells treated with PNA3 NPs and PNA5 NPs (2.5 nmol PNA equivalent dose). mRNA expression levels relative to average control (all normalized to GAPDH, n=3). Data represented as mean  $\pm$  SEM, one sample t and Wilcoxon test were used for statistical analysis.

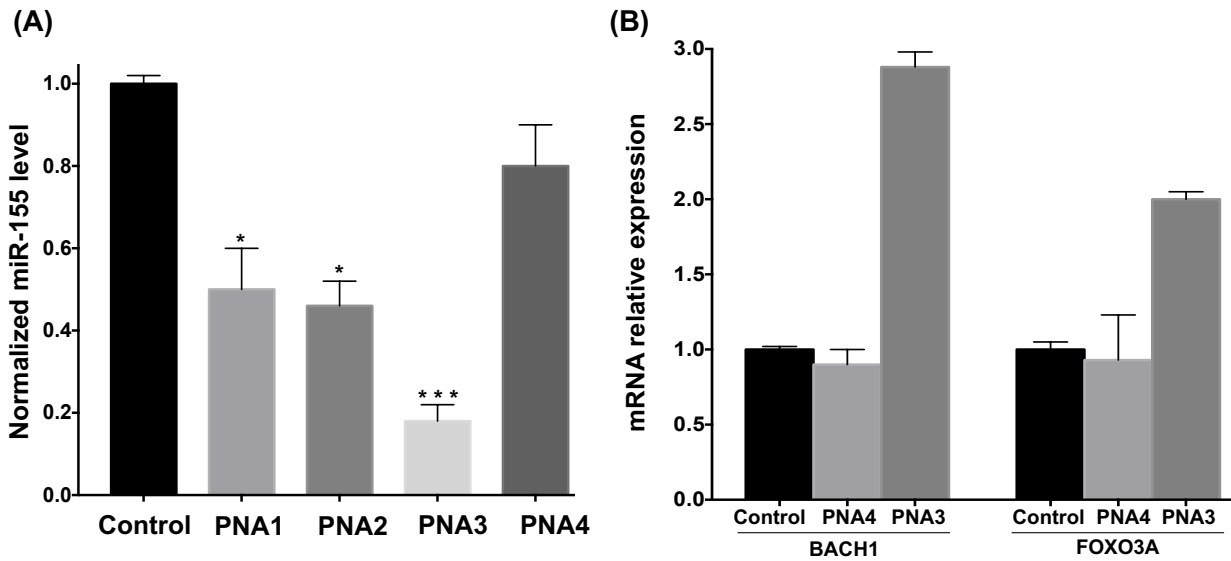


**Figure S15.** (A) miR-155 expression in SUDHL-5 cells after treatment with equivalent PLGA NPs (4 mg) containing PNAs1-4. miR-155 expression relative to average control (all normalized to U6,  $n = 3$ ,  $*p < 0.05$ ,  $*** < 0.0005$ ). (B) Similarly, gene expression level of miR-155 regulated downstream targets; BACH1 and FOXO3A were analyzed in SUDHL-5 cells treated with PLGA NPs (4 mg/ml) containing PNA3 (perfect match) and PNA4 (scramble). Data represented as mean  $\pm$  SEM, one sample t and Wilcoxon test was used for statistical analysis.

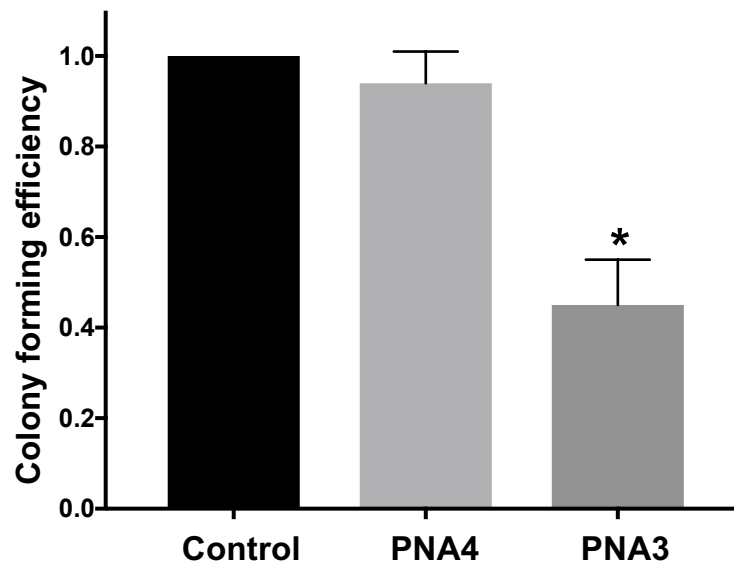


**Figure S16.** Clonogenic assay results. Colony forming efficiency from clonogenic survival assays indicate that pretreatment of cells with PLGA NPs (4 mg/ml) containing PNA3 (perfect match) results in a decrease in survival compared to PNA4 (scramble) and control. N=3, data represented as mean  $\pm$  SEM, one sample t and Wilcoxon test was used for statistical analysis (\*  $p < 0.05$ ).

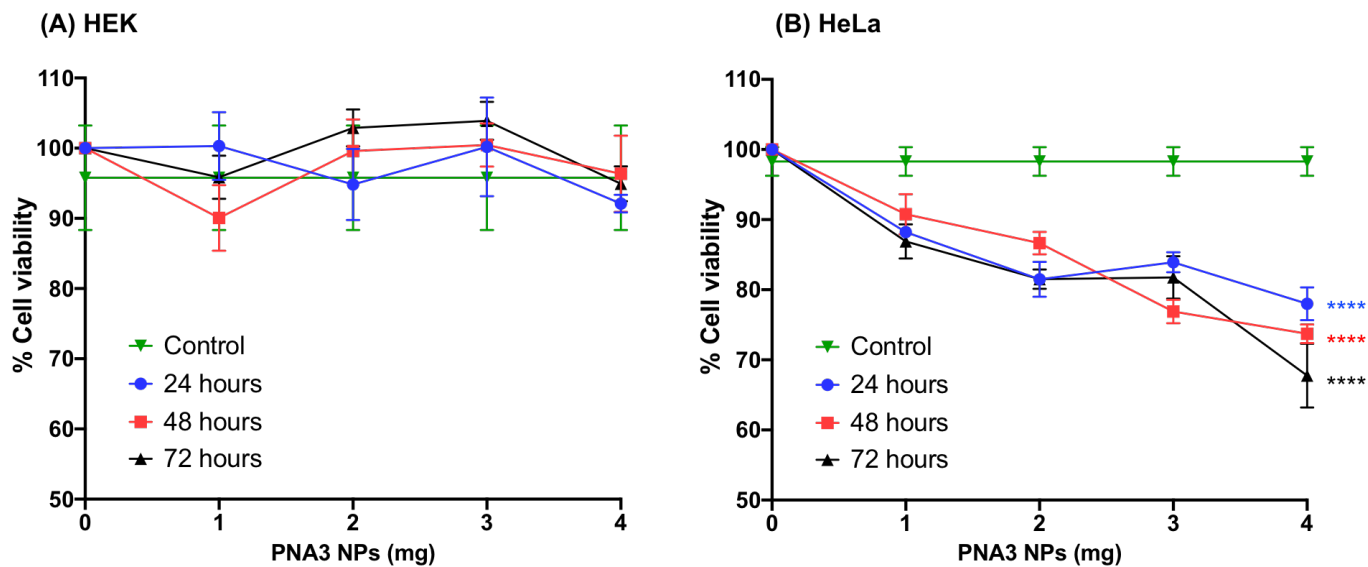


**Figure S17.** (A) Dose dependent effect of PNA3 NPs on cell viability of HEK cells after 24, 48, and 72 hours of incubation. (B) Dose dependent effect of PNA3 NPs in HeLa cells after 24, 48 and 72 hours of incubation. Cell viability measured using MTT assay (n>4, data represented as mean  $\pm$  SEM). For statistical analysis student t test was used (\*\*\*\*p<0.0001).

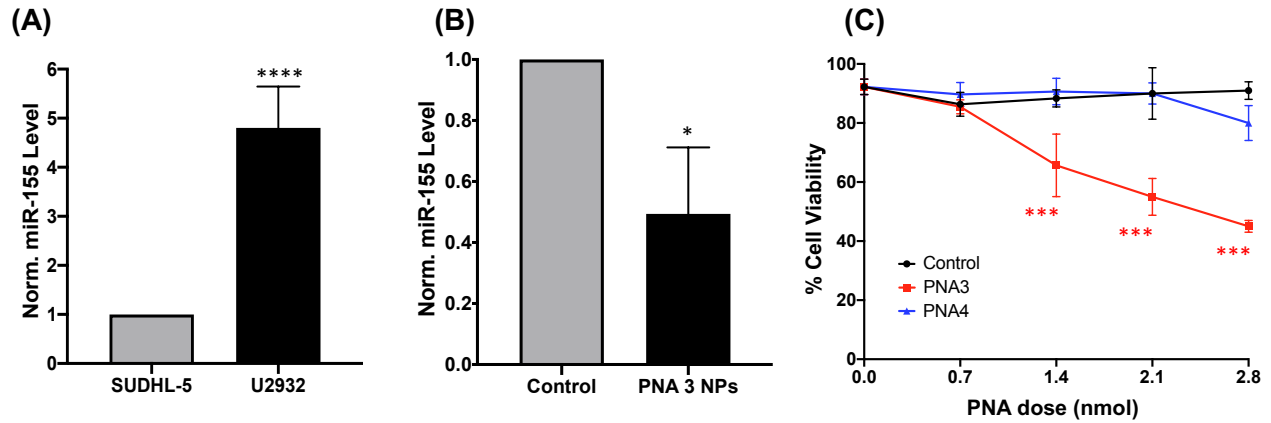


**Figure S18.** (A) miR-155 gene expression in U2932 cells relative to SUDHL-5 cells. (B) miR-155 gene expression in U2932 cells after treatment with PLGA NPs containing PNA3 (2.5 nmol). miR-155 expression relative to average control (all normalized to U6,  $n = 3$ ,  $*p < 0.05$ ,  $****p < 0.0005$ ). One sample t and Wilcoxon test was used for statistical analysis. (C) Dose dependent cell viability assay in U2932 cells after treatment with PLGA NPs containing PNA3 and PNA4.  $n = 3$ ,  $***p < 0.0001$ , multiple t test was used for statistical analysis.



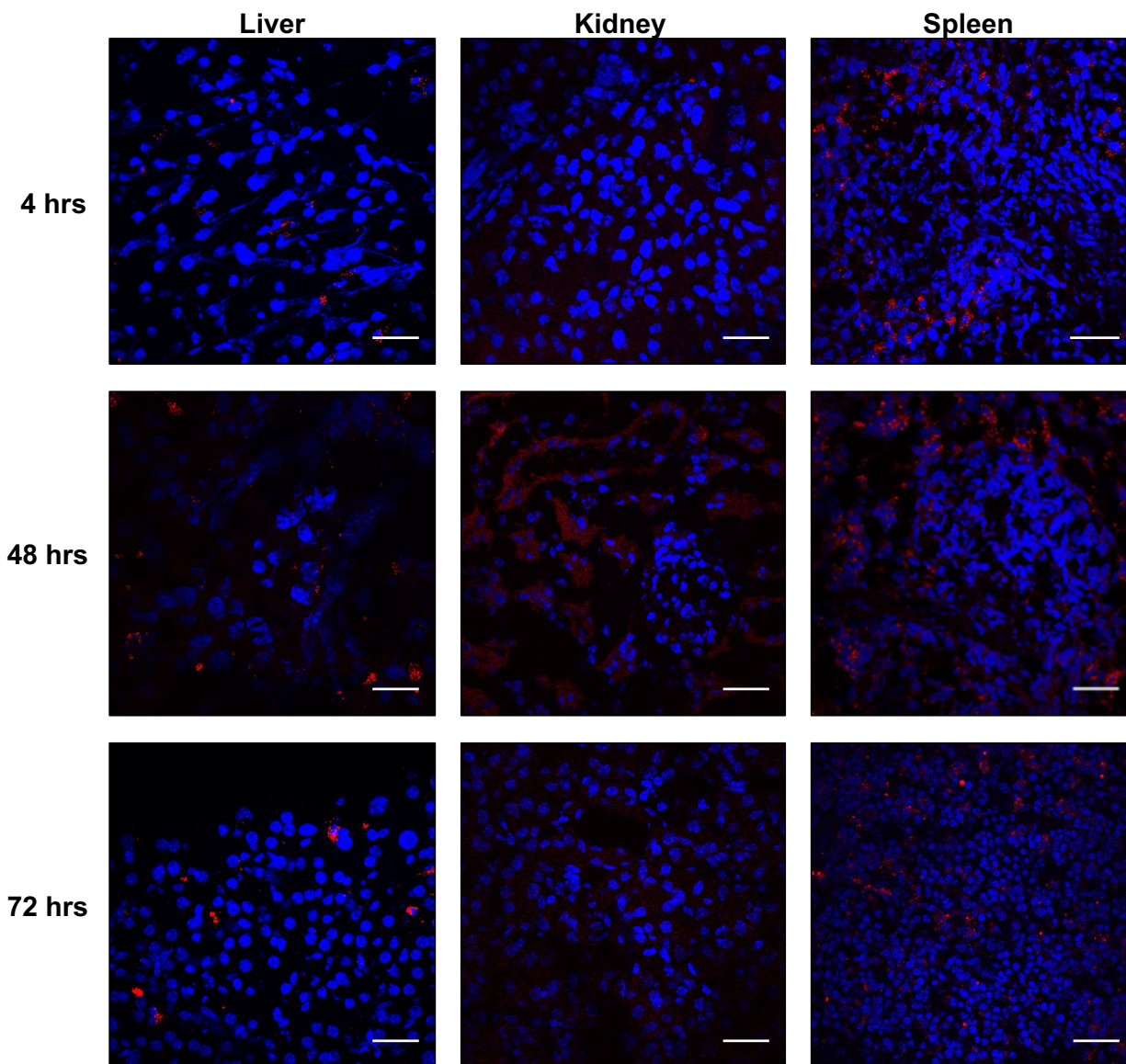


**Figure S19.** The biodistribution of PLGA NPs containing TAMRA PNA in liver, kidney and spleen of mice after 4, 48, and 72 hours of systemic administration. Blue indicates DAPI (nucleus) and red indicates TAMRA. The scale bar represents 30  $\mu\text{m}$ .

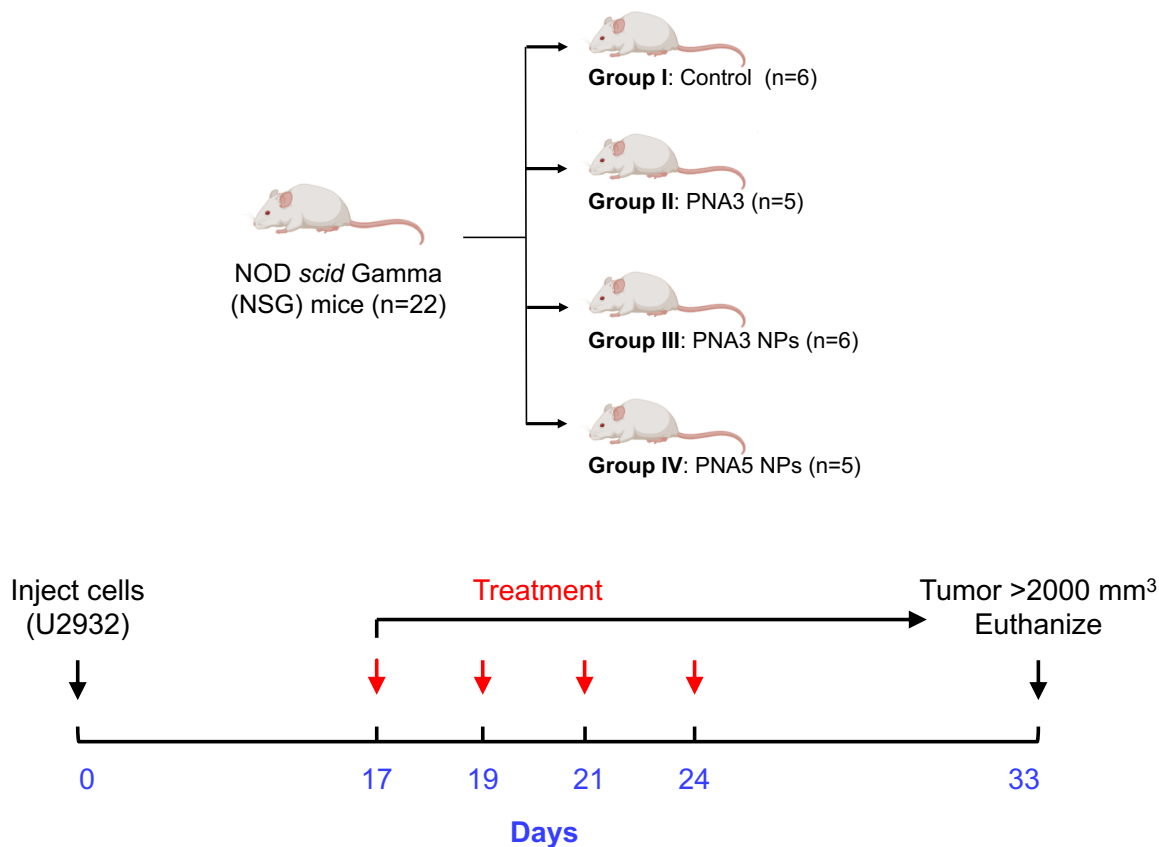


**Figure S20.** Schematic of *in vivo* efficacy studies in immunocompromised mice. Xenograft tumors were established by implanting  $1 \times 10^7$  U2932 cells subcutaneously in the right flank of mice. When the tumor volume reached  $>100 \text{ mm}^3$ , mice were treated with either PBS (control), PNA3, PNA3 NPs, and PNA5 NPs via tail vein injection at 17, 19, 21 and 24 days. Mice in all groups were euthanized when the tumor volume reached  $>2000 \text{ mm}^3$ .

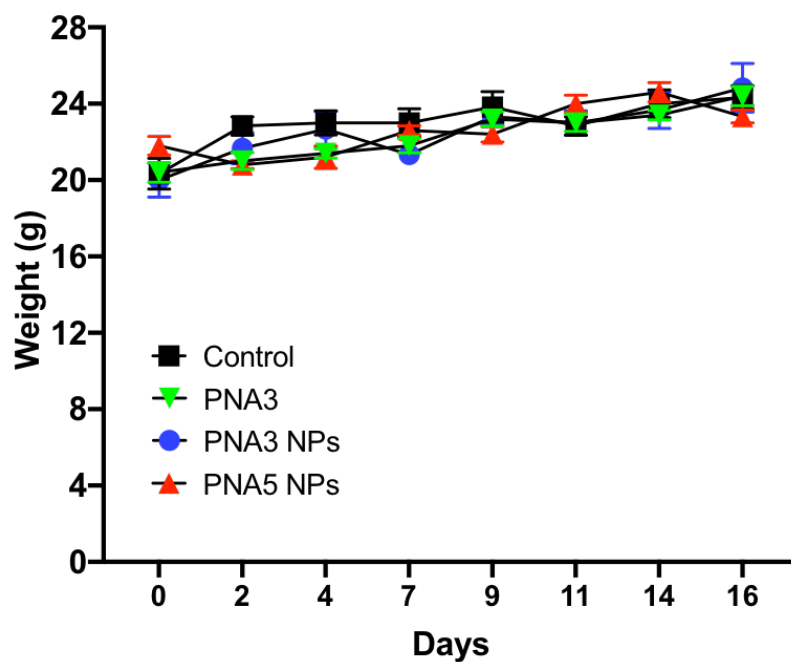


**Figure S21.** Graph representing the weight of NSG mice during the efficacy study. The results are presented as mean  $\pm$  SEM ( $n \geq 5$ ). We did not observe any change in weights of the mice during the study.

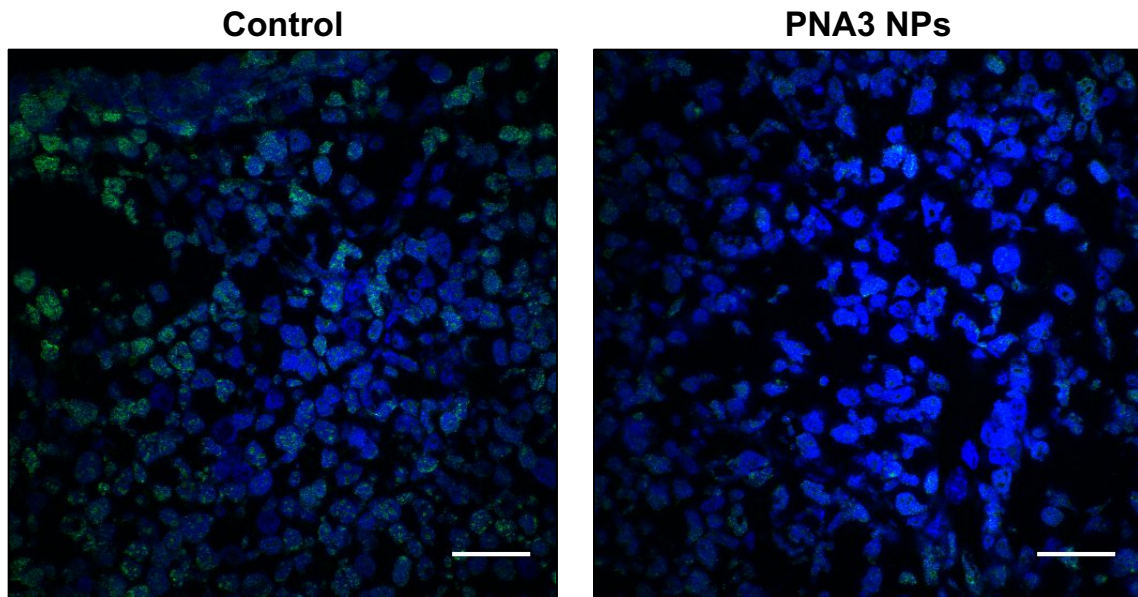


**Figure S22.** Fluorescent images representing Ki67 staining (Green) in control and PNA3 NPs treated tumors. Nucleus (Blue) is stained with DAPI. Scale bar represents 30 $\mu$ m. Control tumor sample shows high Ki67 staining indicating higher proliferation of tumors cells in comparison to the tumor treated with PNA3 NPs which shows minimal Ki67 staining.

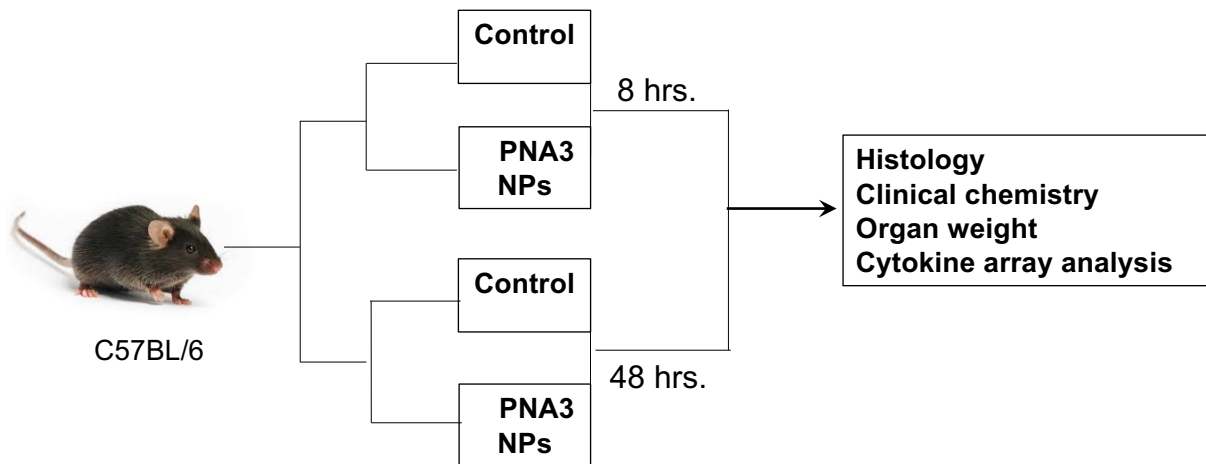
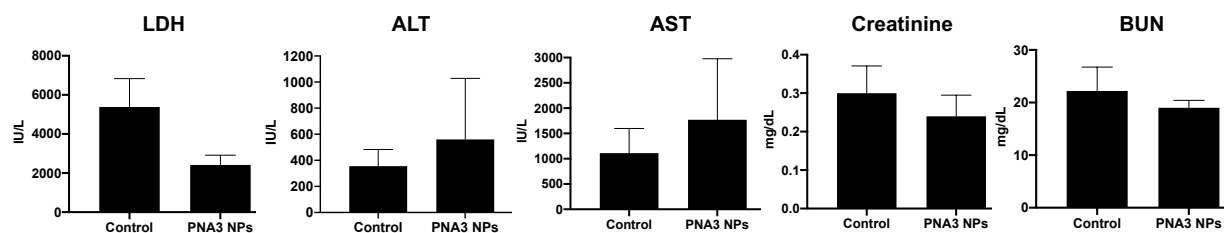


**Figure S23.** Schematic showing experiment performed on wild type immunocompetent mice. Mice were treated with control (vehicle treated) and PLGA NPs containing PNA3. Mice were euthanized after 8 hour and 48 hours of treatment. Clinical chemistry, organ weight, blood chemistry analysis as well as cytokine array analysis were performed.

**(A) Acute toxicity (8 hrs.)**



**(B) Chronic toxicity (48 hrs.)**

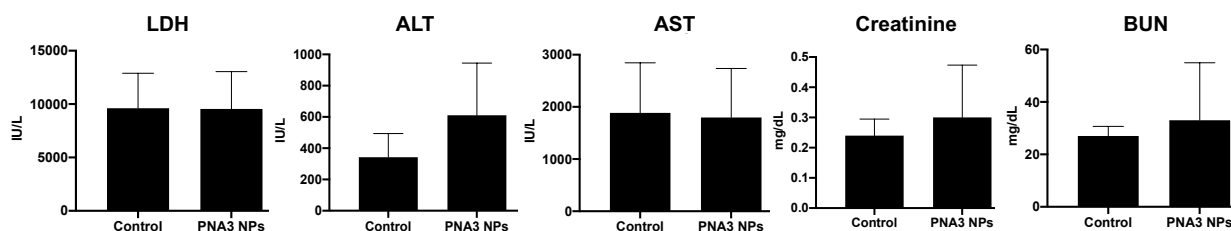


**Figure S24.** Toxicology assessment of intravenously administered PLGA NPs containing PNA3. **(A)** Blood chemistry analysis after 8 hours (acute toxicity) of systemic administration of PLGA NPs containing PNA3. **(B)** Blood chemistry analysis after 48 hours (chronic toxicity) of systemic administration of PLGA NPs containing PNA3. Serum-based clinical chemistry evaluation of systemic toxicity with focus on liver and kidney function. (LDH: Lactate Dehydrogenase, ALT: Alanine Aminotransferase, AST: Aspartate Amino transferase, BUN: Blood Urea Nitrogen). N=5 samples were used and data is represented as mean  $\pm$  SEM.

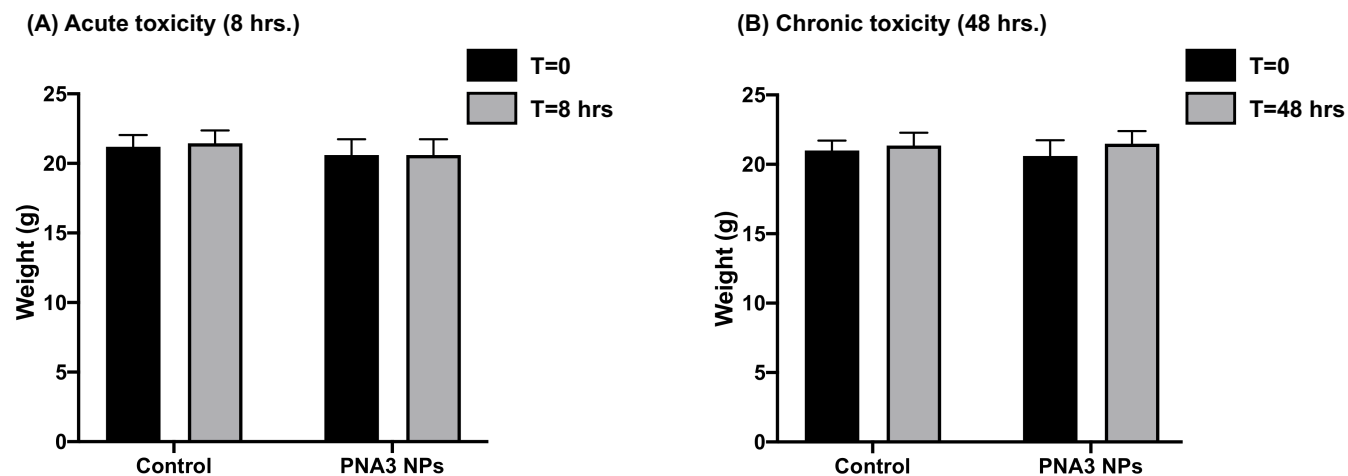


**Figure S25.** (A) Graph representing the weight of C57BL/6 mice at the start (T=0) and end of the acute toxicity study (T=8 hours) in control and PNA3 NPs group. (B) Graph representing the C57BL/6 mice weights at the start (T=0) and end of chronic toxicity study (T=48 hours) in control and PNA3 NPs group. The results are presented as mean $\pm$  SD (n=5). We did not observe any change in mice weights during the study in control as well as PNA3 NPs treated group.

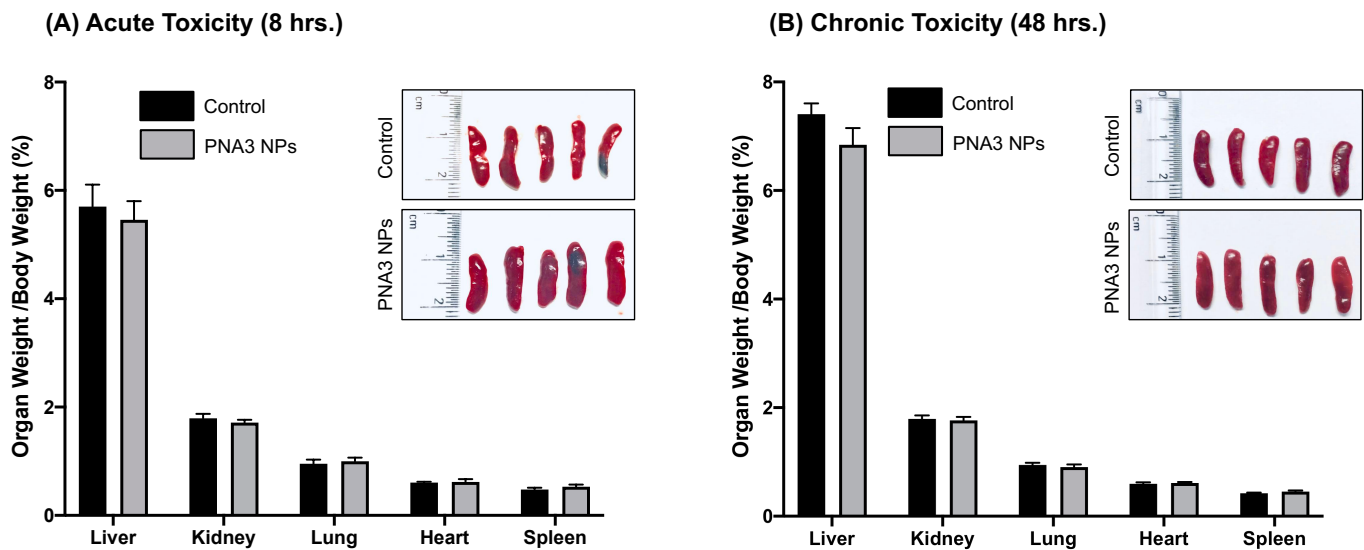


**Figure S26.** (A) Organ mass normalized to total body mass at the time of harvest after 8 hours of treatment with mock buffer (PBS) and PLGA NPs containing PNA3. N=5 samples were used and data is represented as mean  $\pm$  SEM. The inset picture represents the spleen of mice (n=5) in control and PNA3 NPs group. We did not observe any enlargement of spleen between control and PNA3 NPs treated mice. (B) Organ mass normalized to total body mass at time of harvest after 48 hours of treatment with mock buffer (PBS) and PLGA NPs containing PNA3. N=5 samples were used and data is represented as mean  $\pm$  SEM. The inset picture represents the spleen of mice (n=5) in control and PNA3 NPs group. We did not observe any enlargement of spleen between control and PNA3 NPs treated mice.



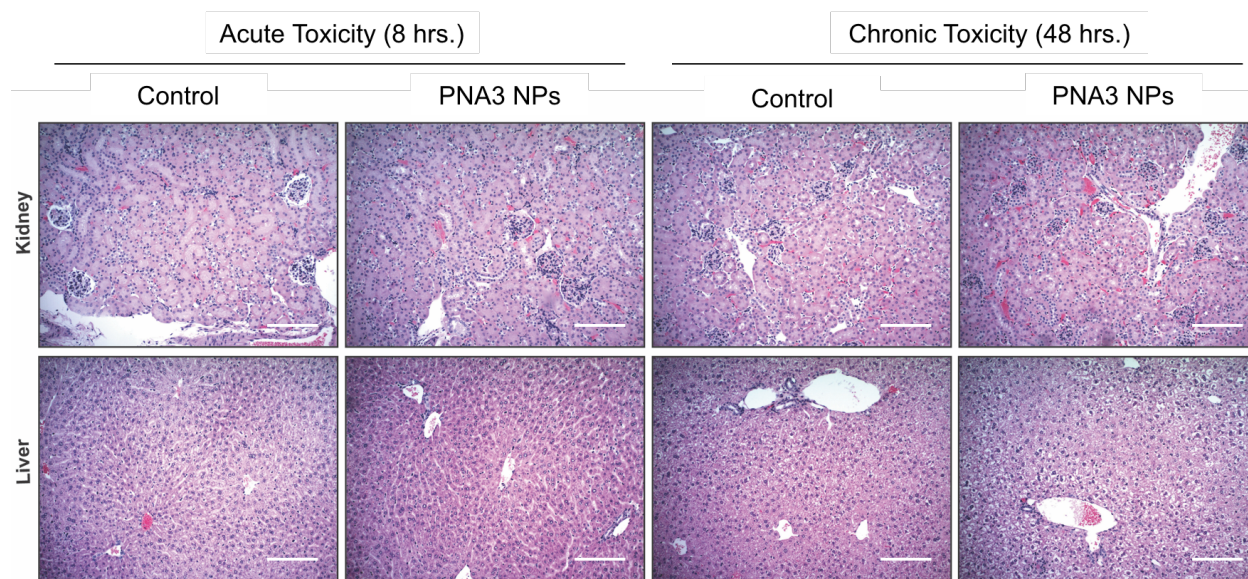


**Figure S27.** H & E staining in kidney and liver of C57BL/6 mice (n=5/group) treated with mock (PBS) buffer and PLGA NPs containing PNA3 show no histologic differences after 8 and 48 hours of treatment. Scale bar represents 200  $\mu$ m.

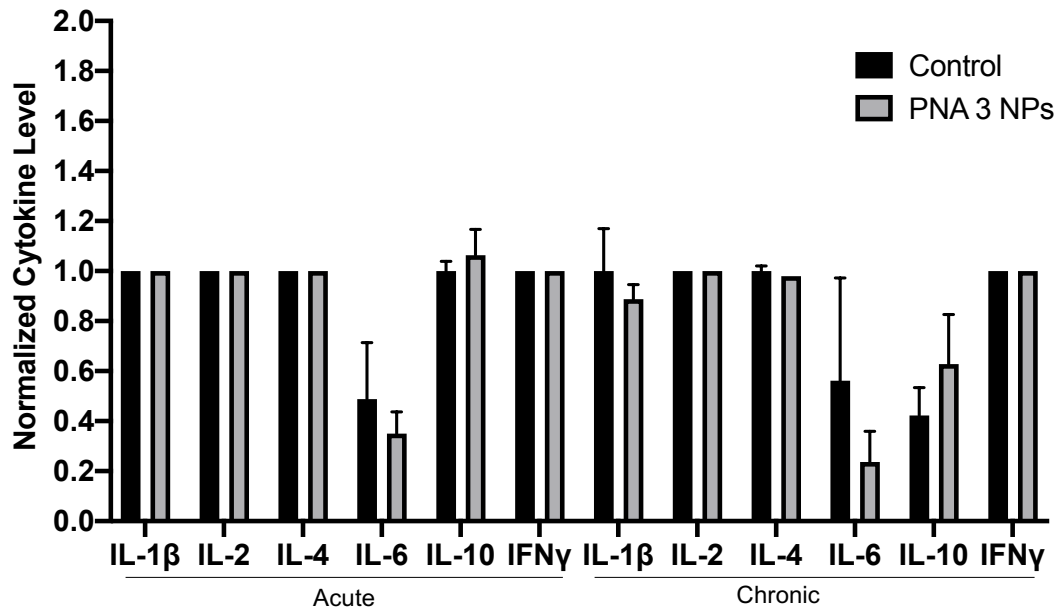


**Figure S28.** Normalized cytokine array detecting the proinflammatory cytokines in the plasma of mice injected with either mock buffer (PBS) or PLGA NPs containing PNA3. Please note that some proinflammatory cytokines were present below the detection limit (0.46 picogram) and hence no marked difference in error bar was noticed. (Acute: 8 hours post-treatment, Chronic: 48 hours post-treatment). N=3 samples were used and data is represented as mean  $\pm$  SEM.

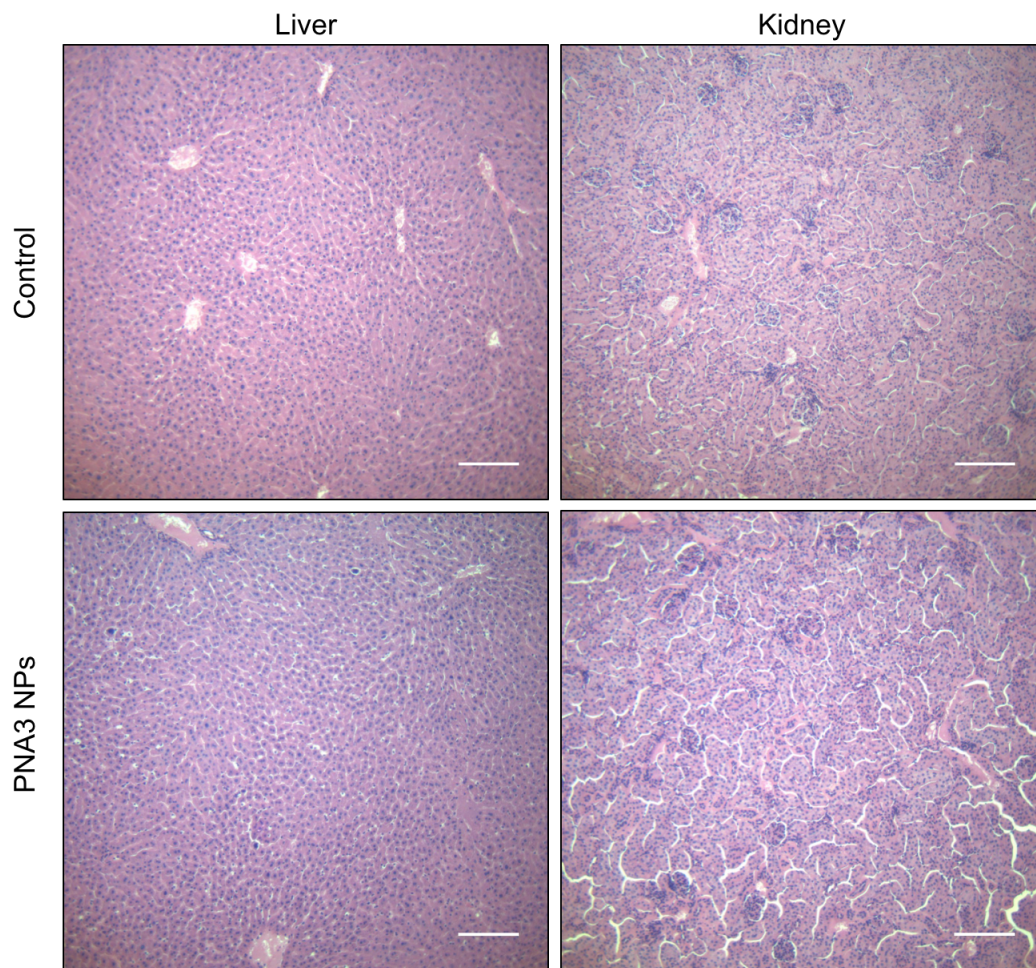


**Figure S29.** H & E staining in liver and kidney of NSG mice (n=6/group) treated with mock (PBS) buffer and PLGA NPs containing PNA3 at the end of efficacy study. The staining shows no histologic differences in treated and control tissues indicating the safety of PNA3 NPs. Scale bar represents 200  $\mu\text{m}$ .